PCCP

Dynamic Article Links

Cite this: *Phys. Chem. Chem. Phys.*, 2012, **14**, 4780–4788

www.rsc.org/pccp

PAPER

Losartan's affinity to fluid bilayers modulates lipid–cholesterol interactions

A. Hodzic,[ab] P. Zoumpoulakis,[c] G. Pabst,[a] T. Mavromoustakos*[d] and M. Rappolt*[a]

Received 13th January 2012, Accepted 16th February 2012
DOI: 10.1039/c2cp40134g

Losartan is an angiotensin II receptor antagonist mainly used for the regulation of high blood pressure. Since it was anticipated that losartan reaches the receptor site *via* membrane diffusion, the impact of losartan on model membranes has been investigated by small angle X-ray scattering. For this purpose 2–20 mol% losartan was incorporated into dimyristoyl-phosphatidylcholine (DMPC) and palmitoyl-oleoyl-phosphatidylcholine (POPC) bilayers and into their binary mixtures with cholesterol in the concentration range of 0 to 40 mol%. Effects of losartan on single component bilayers are alike. Partitioning of losartan into the membranes confers a negative charge to the lipid bilayers that causes the formation of unilamellar vesicles and a reduction of the bilayer thickness by 3–4%. Analysis of the structural data resulted in an estimate for the partial area of losartan, $A_{Los} \approx 40$ Å^2. In the presence of cholesterol, differences between the effects of losartan on POPC and DMPC are striking. Membrane condensation by cholesterol is retarded by losartan in POPC. This contrasts with DMPC, where an increase of the cholesterol content shifts the partitioning equilibrium of losartan towards the aqueous phase, such that losartan gets depleted from the bilayers from 20 mol% cholesterol onwards. This indicates (i) a chain-saturation dependent competition of losartan with lipid–cholesterol interactions, and (ii) the insolubility of losartan in the liquid ordered phase of PCs. Consequently, losartan's action is more likely to take place in fluid plasma membrane patches rather than in domains rich in cholesterol and saturated lipid species such as in membrane rafts.

1. Introduction

Hypertension is the primary risk factor associated with cardiovascular diseases, and the first leading cause of death in economically developed countries.[1] Thus, effective and novel drugs are desired, which can regulate the blood pressure with longer duration of action and fewer side effects. The most important system which interferes with hypertension is the Renin–Angiotensin–Aldosterone System (RAAS).[2] The active product of the RAAS is the hormone angiotensin II (Ang II), which causes vasoconstriction when it binds to the angiotensin subtype 1 receptor (AT_1R). Blockade of AT_1Rs causes vasodilation and reduces the secretion of vasopressin and aldosterone, the combined effect of which is the reduction of blood pressure. Research efforts have been therefore focused on the control of hypertension by blocking the Ang II binding to AT_1R.[3] These efforts were crowned by the approval of losartan in April 1995 by the U.S. Food and Drug Administration (FDA) as the first non-peptide orally active antihypertensive drug in this new class of AT_1R antagonists.[4–6] Since then various non-peptide AT_1R antagonists,[7–9] also known as angiotensin receptor blockers (ARBs), have been marketed with azilsartan medoxomil, a new benzimidazole derivative drug, the last approved by the FDA in February 2011[10] (the European Medicines Agency (EMA) license was authorized in December 2011).

Losartan as a prototype of ARBs belongs to a group of drugs generally classified as sartans. They are amphiphilic molecules, designed to mimic the C-terminal part of Ang II and exert their activity by blocking the binding of Ang II to the AT_1R. Losartan became the lead substance in the development of further AT_1R antagonists, whose common structure is characterized by a biphenyl system to which an acidic moiety is attached, preferentially a tetrazole ring (Fig. 1). Losartan favors a low-energy conformation (see ref. 11 and therein) in

[a] *Institute of Biophysics and Nanosystems Research, Austrian Academy of Science, 8042 Graz, Austria. E-mail: michael.rappolt@elettra.trieste.it; Fax: +39 040 375 8029; Tel: +39 040 375 8708*
[b] *Research Center Pharmaceutical Engineering GmbH, 8010 Graz, Austria*
[c] *Institute of Organic and Pharmaceutical Chemistry, National Hellenic Research Foundation, 11635, Athens, Greece*
[d] *University of Athens, Department of Chemistry, Laboratory of Organic Chemistry, Zographou 15771, Athens, Greece. E-mail: tmavrom@chem.uoa.gr; Fax: +30 2107274761; Tel: +30 2107274475*

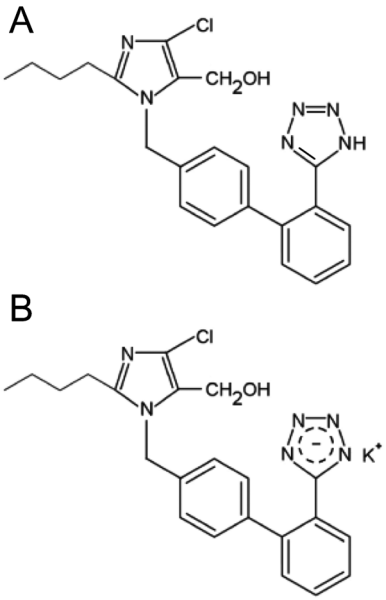

Fig. 1 Chemical structures of losartan (A), and losartan-potassium (B).

which the imidazole and tetrazole rings are placed on opposite sides relative to the spacer phenyl ring plane. The hydroxymethyl group is placed away from the spacer phenyl ring, the alkyl chain is oriented above the spacer phenyl ring, and the two phenyl rings deviate by approximately 60° from being coplanar. Note, about 14% of administered losartan is converted to the active metabolite (EXP3174) by carboxylation,[8] which as an insurmountable antagonist has in comparison to losartan even a 10 times higher affinity for AT_1R.[8]

ARBs are thought to act on the AT_1R by a two-step process.[11] In the first step the incorporation of the drug into the membrane and its diffusion to the receptor site take place; in the second step it binds to the active site pocket of AT_1R.[12,13] Recently also the membrane binding of Ang II was studied by small angle neutron scattering,[14] and it was concluded that the peptide adsorption to the membrane surface may contribute to the binding of Ang II in the active site of the receptor. In this view, biological membranes play an essential role by constituting the first interaction site for drugs to exert their biological action *via* membrane mediated mechanisms. Numerous studies have therefore been performed on sartan–membrane interactions using model membranes mimicking the plasma cell membrane (for review see ref. 15). These include Differential Scanning Calorimetry (DSC),[11,16,17] Electron Spin Resonance (EPR),[16,17] Raman spectroscopy,[18,19] Nuclear Magnetic Resonance (NMR),[18,20,21] molecular modeling,[19,22–24] and X-ray scattering.[19,24,25] For example, DSC results have shown that losartan sensitively affects the chain-melting behavior of dimyristoyl-phosphatidylcholine (DMPC) and dipalmitoyl-phosphatidylcholine (DPPC) membranes.[11,16] Further, EPR spectroscopy revealed that DMPC and DPPC bilayers restrict losartan's motion both in the gel and the fluid phase,[16] indicating a location of the antagonist within the region of the polar–apolar interface of the phosphatidylcholine membrane monolayers. This membranous location of losartan has been further confirmed by NMR studies.[18,21] In general, all studied sartans are found to perturb the membrane structure, phase transition behavior, and membrane fluidity.[26–29] However, the degree of the membrane perturbation varies for the different ARBs.[30] For instance, valsartan and losartan have a strong dose dependent impact on the transition temperature and enthalpy and are known to decrease the chain fluidity above the main phase transitions.[11,17] In contrast, recent Raman spectroscopy investigations on olmesartan displayed an increase of chain fluidity above the melting point, while only relatively small thermal effects were observed,[25] nonetheless olmesartan has a relative high efficacy among the sartans.[30]

In this work we studied by Small Angle X-ray Scattering (SAXS) the influence of losartan (0–20 mol%) on saturated and monounsaturated PC bilayers, and furthermore, investigated the influence of cholesterol in the concentration range of 0 to 40 mol%. The prepared model membranes (liposomal dispersions) were chosen to mimic the plasma membranes of vascular smooth muscle cells, in which AT_1Rs are present and mediate the contractile and hypertrophic effects of Ang II.[3] We note that saturated phosphatidylcholines are the most abundant lipid species in the plasma membrane of the vasculature (40–65%),[31] and that cholesterol's role is essential in establishing proper permeability and fluidity in cell plasma membranes.[32–34] It is well known that cholesterol is responsible for the induction of the liquid-ordered phase (L_o),[35,36] in which the lipids display ordered chains, but nonetheless, are free to diffuse laterally in the membrane monolayer. The L_o phase is assumed to be connected to membrane rafts, functional platforms that enable the assembly of signaling proteins or transbilayer transport, although direct extrapolation from L_o phase properties to membrane rafts is problematic.[37] It is therefore of interest to study the effect of losartan on lipid–cholesterol interactions, and we found a pronounced correlation between the composition of the model membranes and the partitioning of the drug.

2. Materials and methods

2.1 Sample preparation

All lipids were purchased from Avanti Polar Lipids (Birmingham, AL), and used without further purification. Losartan (Los) was provided by Merck (Darmstadt, Germany). Lipid, cholesterol (Chol) and losartan stock solutions were prepared by dissolving weighted amounts of dry lipid, cholesterol and losartan powder in chloroform. The drug concentrations used for the cholesterol-free samples were $x = 0.02$ (2 mol% losartan), $x = 0.05$, $x = 0.10$ and $x = 0.20$. In the PC–Chol–Los bilayer systems the cholesterol concentrations were 3, 5, 20 and 40 mol% at a fixed losartan concentration of 2 mol%. The organic lipid–losartan or lipid–cholesterol–losartan solutions were obtained by mixing appropriate amounts of the stock-solutions, which were then evaporated at room temperature under a gentle stream of nitrogen and thereafter placed under vacuum for 12 hours in order to form a thin lipid film on the bottom of glass vials. The dry lipid films were subsequently re-suspended in 18 MΩ cm^{-1} water (UHQ PS, USF Elga, Wycombe, UK) at a final concentration of 50 mg mL^{-1} and incubated for 4 hours at 45 °C (for the cholesterol series) and 50 °C (for the losartan series) applying vigorous intermittent vortex mixing.

2.2 Microscopy

Optical phase contrast microscopy on DMPC and palmitoyl-oleoyl-phosphatidyl-choline (POPC) vesicles containing losartan was carried out at room temperature using an Olympus SZX12 type microscope equipped with an Olympus DP-10 digital CCD camera (Tokyo, Japan).

2.3 Small angle X-ray scattering

SAXS experiments were carried out at the Austrian SAXS beamline (Elettra Laboratory, Sincrotrone Trieste, Italy).[38] A linear one-dimensional gas detector was used covering the q range ($q = 4\pi\sin\theta/\lambda$; where 2θ is the scattering angle and $\lambda = 1.54$ Å, the selected X-ray wavelength) between 0.01 and 0.6 Å^{-1}. The angular dependence of the scattered intensity was calibrated with silver behenate ($d = 58.38$ Å). The instrumental resolution was determined to have a full width at half maximum of $\delta q = 2.23 \times 10^{-3}$ Å^{-1}. The lipid dispersions were measured in quartz glass capillaries (diameter 1 mm) and thermostated in a custom-built sample holder, which was connected to a circulating water bath (Unistat CC, Huber, Offenburg, Germany). Samples were equilibrated before exposure for a period of 10 min. Exposure times were 2–3 min. Background corrected SAXS patterns were analyzed in the full q-range allowing the application of the modified Caillé theory. The technique and underlying premises have been described previously in detail[39,40] and for reviews see ref. 41–43. The bilayer model used and its applications have been recently presented.[44] From the fits to the scattered intensities $I = S(q)|F(q)|^2/q^2$ ($S(q)$: structure factor; $F(q)$: form factor) we directly obtained the lamellar repeat distance d and the headgroup-to-headgroup thickness, d_{HH}. The width σ_H of the Gaussian peak applied to the model electron density profile of the headgroup region was fixed to 3 Å. Note that steric bilayer thicknesses are not explicitly discussed in this work, but can easily be obtained by *e.g.* applying the equation $d_B = d_{HH} + 4\sigma_H$.[40]

The lateral area per molecule, *i.e.* including lipids and losartan, was determined from

$$A(x) = \frac{2V(x)}{d_{\text{Luzzati}}(x)} \approx \frac{2V(x)}{d_{HH}(x)}, \qquad (1)$$

where x is the inserted molecule concentration of losartan or cholesterol, respectively, V is the effective molecular volume (see below eqn (3)) and d_{Luzzati} is the membrane thickness that is defined by the Gibbs dividing surface.[45] Note that for pure PC bilayers in the fluid phase d_{Luzzati} has nearly the same value as d_{HH}.[46] The influence of insertion of losartan and/or cholesterol into the bilayers on the Gibbs dividing surface was not considered. In the case of a linear dependence of $A(x)$ one can extract estimates for the partial molecular areas A_{PC} and A_{Los} by the relation:[47]

$$A(x) = xA_{Los} + (1 - x)A_{PC} \qquad (2)$$

The effective volumes of DMPC–Chol and POPC–Chol bilayer systems have been recently published, and further experimental details are described in ref. 33. For the studied binary PC–Los and ternary PC–Chol–Los formulations the effective volumes were estimated using:

$$V(x) = xV_{Los} + (1 - x)V_{PC} \qquad (3)$$

with $V_{Los} = 522$ Å^3 (the bare volume was estimated from losartan's density in the solid state $\rho = 1.341$ g cm^{-3}[6] and its molecular weight $M_W = 421.9$ g mol^{-1}), and the values of $V_{DMPC} = 1103$ Å^3 ($T = 35$ °C) and $V_{POPC} = 1250$ Å^3 ($T = 25$ °C) are taken from ref. 33. Application of the bare volume of losartan assumes that insertion of losartan does not lead to a condensation of the membrane. If condensation takes place, then V_{Los} is expected to become smaller than 522 Å^3.[48]

3. Results

3.1 Behavior of PC–Losartan bilayers

The influence of losartan (Fig. 1) on the structural properties of fluid phospholipid bilayers composed of saturated and monounsaturated lipids, respectively, has been investigated by SAXS. The experiments have been carried out at 25 °C for POPC samples ($T_m = -3.3$ °C)[49] and at 35 °C for DMPC samples ($T_m = 24$ °C).[50] Fig. 2 demonstrates that already 2 mol% losartan leads to a complete loss of positional correlations between adjacent bilayers. Both the POPC–Los and DMPC–Los samples display a typical bilayer form factor scattering pattern[51,52] without any trace of diffraction peaks (upper scattering curves in Fig. 2A and B). In contrast, both pure PC-bilayer systems show the common small angle X-ray diffraction pattern of multilamellar vesicles (MLVs), as previously published.[33] Membrane unbinding upon the addition of losartan has been further confirmed by optical microscopy. At room temperature the POPC–Los dispersion contains mainly giant unilamellar vesicles (Fig. 2C), and the absence of multilamellar vesicles was checked with crossed polarizers, *i.e.* the image field remained black (not shown). The formation of unilamellar vesicles can be explained by the negative surface

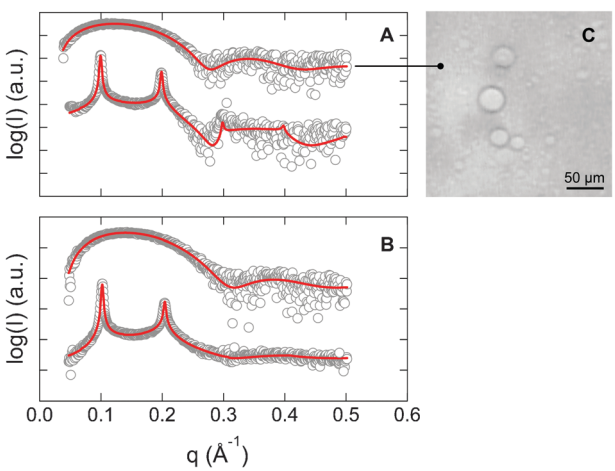

Fig. 2 Effect of 2 mol% losartan incorporation into bilayers of POPC at room temperature and of DMPC at 35 °C. (A) The diffraction pattern of pure POPC bilayers is displayed (bottom) in comparison to the scattering pattern of POPC bilayers containing 2 mol% losartan (top). (B) The diffraction pattern of pure DMPC bilayers is presented (bottom) in comparison to the scattering pattern of DMPC bilayers containing 2 mol% losartan (top). Best fits to the data are given by solid red lines. (C) In the optical microscopy image giant unilamellar vesicles of POPC–losartan are seen. The sample was not birefringent under the polarizing microscope.

charge density conferred to the bilayers upon losartan insertion. It has to be noted that losartan was provided in the form of a potassium salt, and has therefore a negatively charged tetrazole ring (Fig. 1B). Further, due to the low pK_a value of losartan of 2.95–3.14[53,54] practically 100% of the molecules remain negatively ionized also after hydration at neutral pH (ionization fluctuations above 10% are expected for pH values <4). We note further that losartan exhibits in principle a basic centre at the imidazole group with pK_a = 4.2.[53] However, at neutral pH its positive ionization is practically 0, and thus, the basic centre at the imidazole group is not an issue of the present study (remarkable ionization fractions are expected only below pH 5). In respect of observed membrane unbinding also the expected membrane bound fraction of losartan after hydration is of interest. Applying the octanol water partition coefficient of losartan (log P 1.12),[53] this fraction can be estimated to be 93%. However, the true fraction is expected to come close to 100%, since octanol as a non-ionic amphiphile has a smaller binding affinity to losartan as compared to zwitterionic phospholipids (compare also the discussion in Section 4.1).

To get hold on the structural membrane parameters all scattering patterns in this work have been fitted by a global analysis technique (see Materials and methods), allowing the fitting of the SAXS data in the full q-range (red lines in Fig. 2A and B). A summary of the key structural parameters of the POPC–Los (open circles) and DMPC–Los systems (closed circles) *vs*. losartan concentration is given in Fig. 3. The overall effect of losartan on the bilayer thickness is not very big (Fig. 3A). Especially the POPC bilayers display an almost equal headgroup-to-headgroup thickness, d_{HH}, over the entire studied drug concentration range. After a minute bilayer thickening of 0.5 Å (at 2 mol% Los) a continuous thinning of the bilayer from 37.1 to 35.7 Å is observed. The influence of losartan on the DMPC bilayers is a bit more significant, and again after a slight bilayer thickening of 0.9 Å (reached at 5 mol%) a decrease of d_{HH} from 34.7 to 32.5 Å is seen. To summarize, the overall thinning of the POPC bilayers is 3% (referring to changes in d_{HH}/d_0, in which d_0 stands for the headgroup-to-headgroup distance of the pure PC bilayers), whereas the DMPC bilayers thickness decreases by 4%. The effective lateral area per molecule, A, has been estimated using eqn (1) (Fig. 3B). For the pure lipid systems A takes a value of 68 Å^2 for POPC at 25 °C and equals 65 Å^2 for DMPC at 35 °C, respectively, which compares well with literature data. Kucerka *et al*. published for POPC at 30 °C a value of 68 Å^2,[55] and recently, Khelashvili *et al*. reported for DMPC an area per lipid of 63 Å^2 (at 35 °C).[56] Thus, the Luzzati approach for the area calculation (eqn (1): $A(x) = 2V(x)/d_{HH}(x)$) might lead to slightly overestimated molecular area values for DMPC. However, most important in this study is to report on relative changes in membrane properties upon the addition of losartan. As seen in Fig. 3B the effective molecular area decreases monotonously with addition of losartan. This can be explained considering that the effective $A(x)$ is given by the molecular weighted sum of the bare partial areas A_{PC} and A_{Los} (Eq 2). The resulting values are for POPC–Los bilayers $A_{POPC} = 67 \pm 0.5$ Å^2, $A_{Los} = 38 \pm 3.5$ Å^2, and for DMPC–Los bilayers we found $A_{DMPC} = 64 \pm 1$ Å^2, $A_{Los} = 42 \pm 7.5$ Å^2. This means that

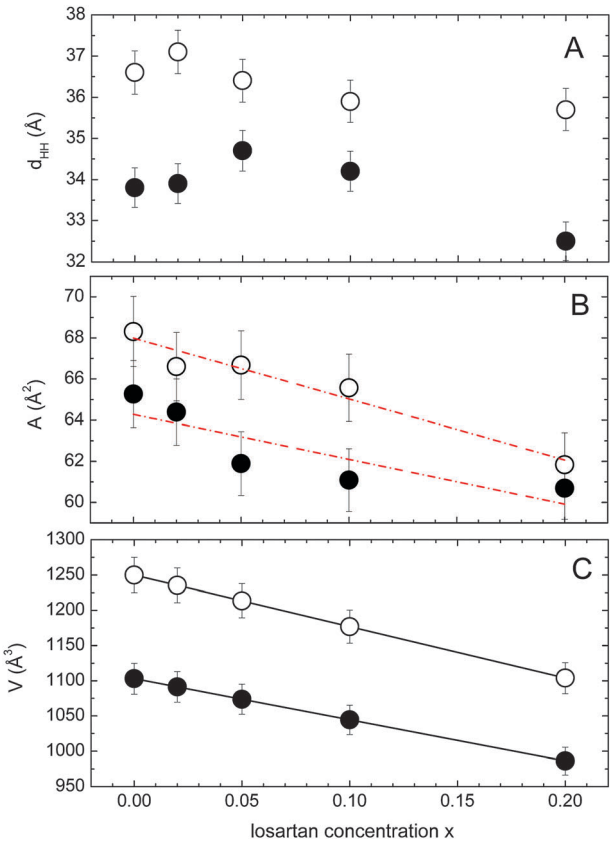

Fig. 3 Losartan concentration dependence of the headgroup-to-headgroup thickness, $d_{HH}(x)$ (A), the effective area per molecule, $A(x)$ (B), and the effective molecular volume, $V(x)$ (C), of the binary mixture of POPC–Los (open circles) and DMPC–Los (solid circles) at 25 and 35 °C, respectively. The straight dash-dotted line in panel B is the best fit to $A(x)$ using eqn (2), and the data in panel C are estimations of $V(x)$ applying eqn (3).

within the error margins the occupied lateral area of losartan in the fluid PC-bilayers is about 40 Å^2. For the estimation of the effective volume (eqn (3)) we also assumed a molecular weighted addition of the bare partial volumes of losartan and PC-lipids, respectively, and determined a relative volume decay of 12% for POPC–Los and 11% for DMPC–Los bilayers, both at a drug concentration of $x = 0.2$ (Fig. 3C).

Taking a closer look at the trend of $A(x)$ (Fig. 3B) the applied method to estimate the bare areas using eqn (2) is at least questionable for the DMPC data, since a linear fit seems inadequate for small values of the losartan concentration, x. Therefore, we considered the partial-specific areas as suggested by Edholm and Nagle.[57] In Fig. 4, the same data have been plotted in the form $A(x)/(1-x)$ *vs*. $x/(1-x)$, which allowed us to extract the specific area of losartan from the slope of the local tangent and the areas of POPC and DMPC, respectively, from the intercept of this tangent at $x = 0$. Data for POPC showed initially a small decrease, followed by a linear increase, while the two linear regimes for DMPC are clearly discernible. The similarity of these data to that from DPPC–Chol mixtures (Fig. 3 in Edholm and Nagle[57]) suggests that losartan causes a condensation of lipid bilayers, analogous to the well-known effect of membrane condensation by cholesterol. From the

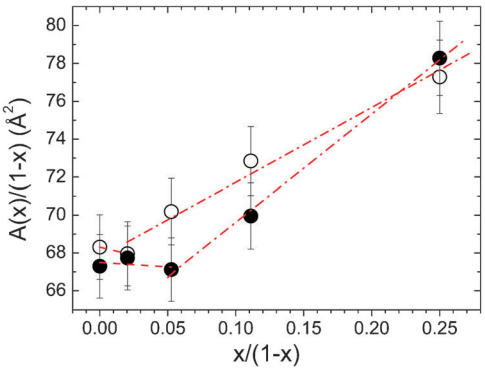

Fig. 4 $A(x)/(1 - x)$ *versus* $x/(1 - x)$ plot. The four straight lines indicate possible fits for small and medium x. Data refer to $A(x)$ in Fig. 3B of binary mixtures of POPC–Los (open circles) and DMPC–Los (solid circles) at 25 and 35 °C, respectively.

local tangent at low x we find negative specific areas for losartan $A_{Los} = -17$ Å^2 in POPC and $A_{Los} = -4$ Å^2 in DMPC. Negative partial areas may appear unusual at first sight, but are typical for the partial-specific area concept, for membrane condensing compounds. Analogously, the effect of electrostriction observed for example in dielectrics leads to negative partial-specific volumes. In this view, which is different from the atomistic view applied in eqn (2) to determine the partial areas, the guest molecules perturb the PC bilayers only locally, so that the partial areas of the POPC or DMPC remain constant in the global average, and the condensation is observed in a negative partial area of losartan. This condensation ability of losartan confirms also the Raman spectroscopy results on DPPC bilayers that evidenced an increase in the ratio of *trans*/*gauche* conformers upon the addition of losartan.[18]

3.2 Losartan's interaction with PC–Chol bilayers

In the second part, we investigated the influence of 2 mol% of losartan on PC–Chol bilayers composed of different PC lipids and varying cholesterol composition. SAXS patterns of fully hydrated vesicles of POPC–Chol at 25 °C and DMPC–Chol at 35 °C with cholesterol concentrations ranging from 3 to 40 mol% are shown in Fig. 5. Nearly all scattering patterns display diffuse scattering only, arising from the form factor contribution of the bilayers. As outlined before, this is explained by the presence of electrostatic repulsion between neighboring membranes due to the incorporation of the negatively charged losartan molecules.

However, at cholesterol concentrations of 20 and 40 mol%, Bragg peaks become visible in the scattering pattern of the DMPC–Chol dispersions (Fig. 5B). Most clearly, at 40 mol% the diffraction pattern reflects that the MLVs have been formed. The interbilayer distance is highly sensitive to the balance of attractive and repulsive forces between adjacent membranes. Hence, the electrostatic force must have decreased drastically in order to allow the formation of membrane stacks. In this high concentration regime of cholesterol an obvious explanation is at hand, if losartan depletion from the DMPC–Chol bilayers would take place and losartan would be preferentially located in the aqueous phase. Alternatively, losartan could bury its charge deep inside the apolar region.

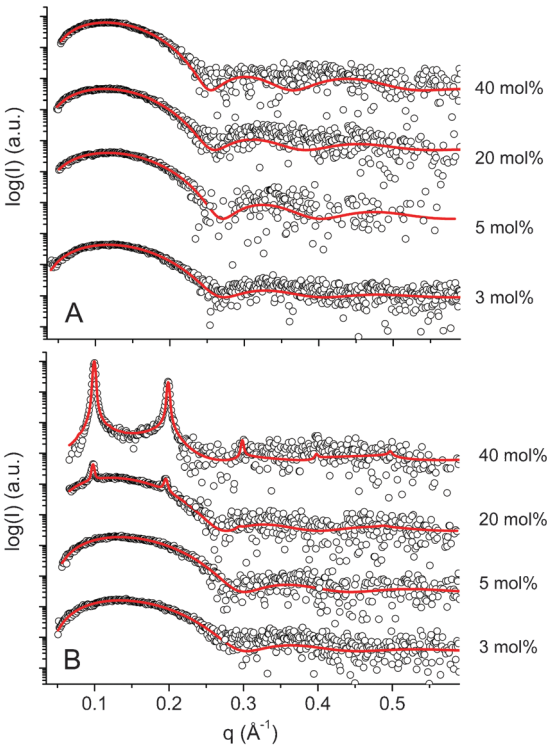

Fig. 5 X-Ray diffraction patterns of fully hydrated multilamellar vesicles of POPC–Los at 25 °C (A), and DMPC–Los at 35 °C (B) with cholesterol concentrations ranging from 3 to 40 mol%. The cholesterol concentrations are indicated on the right hand side of each SAXS pattern. For all samples the losartan concentration was fixed at 2 mol%. The solid lines show the best fit to the data applying a global analysis technique.

However, this is highly unlikely. A closer look to the fitting results (Fig. 6) supports the scenario that losartan gets expelled from DMPC lipid bilayers by cholesterol. While the presence of losartan clearly decreases the headgroup-to-headgroup thickness, d_{HH}, over the whole investigated cholesterol concentration range for the POPC–Chol systems (Fig. 6A), this is not the case for the DMPC–Chol bilayers. At 40 mol% cholesterol concentration d_{HH} of DMPC–Chol and DMPC–Chol–Los bilayers are within the given errors the same (Fig. 6B). Moreover, at this concentration also the measured interbilayer distances in the DMPC–Chol–Los and DMPC–Chol systems are the same: $d - d_{HH} = 63.2 - 39.0 = 24.2$ Å compares to $63.2 - 39.2 = 24.0$ Å (the d-spacings were determined by global fitting of the SAXS pattern, *e.g.* in Fig. 5B).

At concentrations of cholesterol up to 20 mol% in DMPC–Chol bilayers and over the whole studied concentration range of cholesterol in POPC–Chol bilayers the membrane-insertion of losartan results in a significant decrease of the membrane thickness. Membrane thinning is, however, at all cholesterol concentrations significantly more pronounced in POPC–Chol mixtures. For instance at 20 mol% cholesterol concentration, already an inspection by eye makes clear that both the membrane thinning, Δd_{HH}, and concentration offset, Δx (for definitions see Fig. 6A), are greater for POPC membranes (*cf.* Fig 6A with Fig 6B). The effective areas per molecule, $A(x)$ (eqn (1)), are presented in Fig. 6C and D.

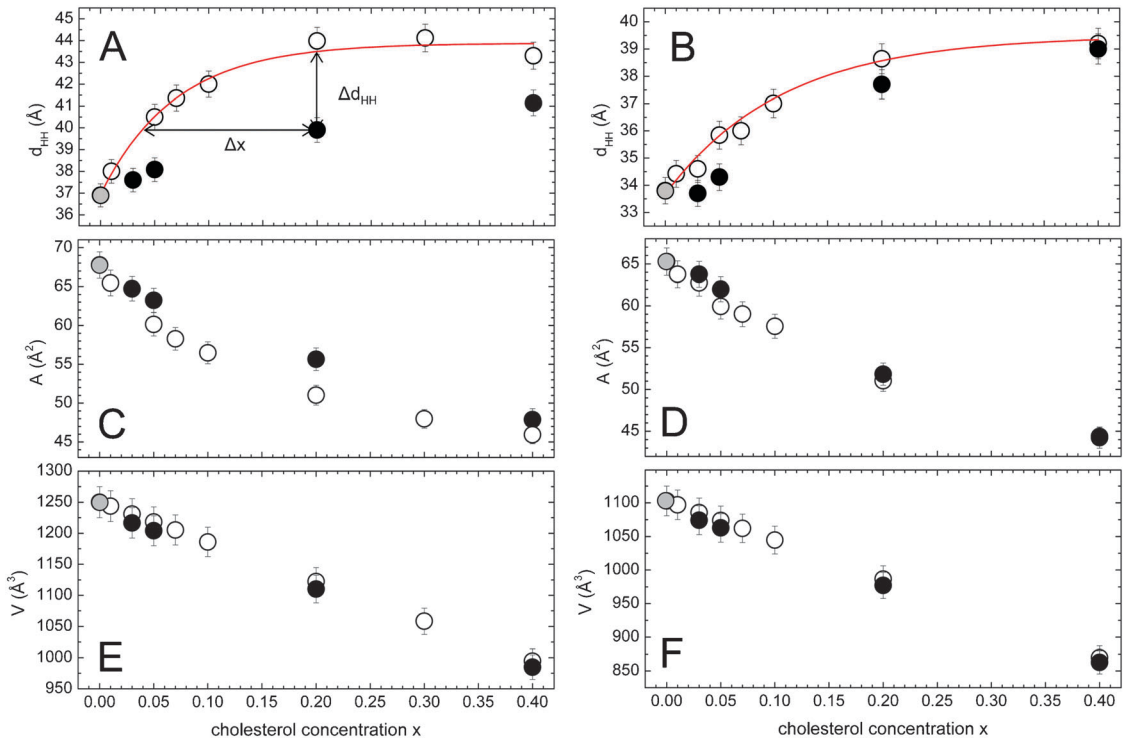

Fig. 6 Bilayer thickness, d_{HH} (A,B), effective area per molecule, A (C,D), and effective volume, V (E,F) values *vs.* cholesterol concentration from binary PC–cholesterol (open circles) and ternary mixtures of PC–losartan–cholesterol (solid circles). The losartan concentration was fixed at 2 mol%. On the left POPC data recorded at 25 °C are presented (A,C,E), and on the right DMPC data at 35 °C are shown (B,D,E). Pure PC–water data are color coded grey. The trends of d_{HH} of the PC–Chol bilayer systems follow an exponential function of first order (red lines). The membrane thinning, Δd_{HH}, and concentration retardation offset, Δx, effect of losartan are defined in panel A for the drug concentration $x = 0.2$. At any given concentration x, $\Delta d_{HH} = |d_{HH}(\text{PC–Chol–Los}) - d_{HH}(\text{PC–Chol})|$, and at any given membrane thickness d_{HH}, $\Delta x = |x(\text{PC–Chol–Los}) - x(\text{PC–Chol})|$. Both Δd_{HH} and Δx were determined with respect to the single exponential fits given for d_{HH} (open circles) (full red lines in panels A and B).

In agreement to the membrane thickness behavior, by increasing the cholesterol concentration a monotonous lipid chain condensation is observed. This effect is hindered by losartan, and again this impediment is stronger expressed for the POPC–Chol bilayers. Last, in Fig. 6E and F the estimated effective volumes per molecule are shown. They are calculated from the partial volumes as specified in the Materials and methods section. Due to the relatively small partial volume, $V_{Los} = 522$ Å^3, and the low concentration of losartan (2 mol%), its effect on the effective volumes of the studied PC–Chol bilayers is rather small.

4. Discussion

4.1 Losartan's interaction with phosphatidylcholines

Numerous experiments confirm the insertion of losartan into phosphatidylcholine bilayers. ^{13}C NMR spectroscopy revealed (i) changes in peak intensity and line-width due to modified membrane fluidity, (ii) changes in chemical shift values of individual carbon nuclei being due to modified phase transition profiles, and (iii) the appearance of a specific subset of peaks corresponding directly to the incorporated drug molecule. For instance an additional peak at 19 ppm was attributed to the C_9 of the butyl chain of losartan, which is apparent in the whole temperature range of 25–45 °C in a DPPC–Los preparation (20 mol% Los).[11,18] DSC results can be summarized as follows: (i) the pretransition of PCs is abolished already at low losartan concentrations, (ii) the main transition temperature and cooperativity decrease with the increasing drug content, and (iii) at very high drug concentrations an enthalpy increase of the main transition was reported for DPPC–Los bilayer systems, where $\Delta H_m = 9.1$ kcal mol^{-1} (Los 20 mol%).[11] A similar behaviour was found for DMPC–losartan interactions: an overall slight enthalpy decrease for drug concentrations from $x = 0$ to 0.10 follows a monotonous enthalpy increase from $x = 0.1$ to 0.5.[16] Last, Raman spectroscopy studies on DPPC–Los bilayers have shown that the *trans* to *gauche* ratio of the lipid chains increases in the gel phase and decreases in the L_α phase.[18] In this sense losartan displays a similar effect to cholesterol: membranes become more fluid in the gel phase and less fluid above the melting point.

These reported thermodynamic and spectroscopic results are complemented by the structural ones that we ascertained in this study by SAXS. For instance a slight chain ordering effect induced by losartan in the L_α phase is also observed. In Fig. 3A a small bilayer thickness increase at low drug concentrations is noticed (+0.5 Å for POPC and +0.9 Å for DMPC). This can be compared to the effect of cholesterol alone: at 2 mol% d_{HH} increases +1.8 Å for POPC and +0.8 Å for DMPC (Fig. 6A and B, open circles). Astonishingly, in the low concentration regime losartan shows a similar membrane

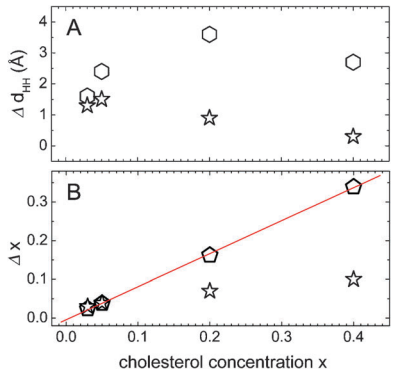

Fig. 7 Losartan's effectiveness in conserving the L_α phase. Losartan (2 mol%) reduces the membrane thickness of PC–Chol bilayers (*cf.* Fig. 6A and B). Referring to the definitions given in Fig. 6A the difference of the headgroup-to-headgroup distance, Δd_{HH}, is given in panel A and the cholesterol concentration offset, Δx, is displayed in panel B. POPC data (pentagon) indicate a stronger membrane thinning effect than DMPC data (star).

condensation power as cholesterol. On a molecular level this ordering effect may be ascribed to electrostatic interactions between the negatively charged tetrazole group and surrounding $N^+(CH_3)_3$ groups of the phospholipids that provide a robust anchor in the lipid–water interface for van der Waals interactions between the butyl alkyl chain and biphenyl group of losartan with the acyl chains of the phospholipids which maximize the amphipathic interactions. This view also coincides with NMR results,[11,29,58] from which losartan is expected to reside around the polar–apolar interface of the membrane leaflets. Thus, losartan's impact on the chain ordering is expected to take place preferentially in the upper hydrocarbon chain region.

However, at higher losartan concentration this chain ordering effect gets obscured, as pointed out in earlier works,[17,19] by the onset of a partial bilayer interdigitation effect, which works in the opposite direction. As an overall effect the d_{HH} values start to decrease at medium values of x (Fig. 3A). From 5 mol% losartan onwards a continuous membrane thinning is seen. Since the overall penetration depth of losartan is significantly smaller than the total lipid monolayer thickness, one opposing lipid–losartan pair in the bilayer is expected to span a shorter distance than two opposing lipids, and hence the overall membrane thickness reduces (see Fig. 3A and the results overview in Fig. 8A and B). Obviously this effect gains in influence with increasing drug concentration, but it is relatively small for losartan when compared to *e.g.* the membrane-thinning effect of valsartan. At a drug concentration of 20 mol% the membrane thickness decreases in fluid PC bilayers 3–4% in the presence of losartan, whereas it reduces around 9% in the presence of valsartan. Also the estimated partial area per losartan molecule is about 40 $Å^2$ relatively small in comparison to the value of 58 $Å^2$ that was found for valsartan.[17]

4.2 Liquid ordered phase insolubility of losartan (and possible consequences)

As outlined in the Results section, the incorporation of losartan into PC–Chol membranes results in a decrease of the bilayer thickness, and we could clearly show that losartan has a stronger influence on monounsaturated than on saturated lipids (Fig. 6A and B). This differing impact of losartan onto POPC–Chol and DMPC–Chol bilayers, respectively, is analyzed in greater detail in Fig. 7. The membrane thinning effect of losartan is identified with its ability to hamper the L_o phase induction by cholesterol. Fig. 7A shows explicitly the much bigger efficiency of losartan to conserve the L_α phase in the POPC based system. On a molecular level we attribute this to the π-orbitals of the C_9 *cis*-double bond of the oleoyl chains, which induce an inflexible chain "kink", and do not fit the hydrophobic rings of cholesterol,[59] while a weak complex formation of the C_9 double bond with the aromatic rings of losartan might take place.[60] The higher affinity of cholesterol for saturated chains is well known.[36,59,61] For instance the (L_α + L_o) to L_o phase boundary for DMPC–Chol bilayers at 35 °C has been reported to be at x = 0.28–0.32, while this phase boundary in POPC–Chol bilayers at 25 °C has been observed at higher x = 0.37–0.46 (see ref. 36 and therein). Additionally, it is tempting to assume that the cholesterol has a higher affinity to saturated chains as compared to losartan. Recalling cholesterol's extensive penetration depth in PC monolayers[56] strengthens this assumption. Consequently, we expect a lower affinity of cholesterol to unsaturated chains as compared to losartan, which we know has a relatively smaller penetration depth in the membrane leaflets, and therefore might be less disturbed by the presence of the C_9 double bond of the oleoyl-chains or, as stated above, even be weakly attracted due to π–π-interactions.[60] Thus, the presence of losartan additionally weakens the ability of cholesterol to induce chain order in the oleoyl chains, and hence would explain the hampered induction of the L_o phase. Fig. 7B displays the concentration offset, Δx (for definition see Fig. 6A), as a function of the cholesterol concentration. Interestingly, for POPC–Chol experiments Δx displays a linear dependence with a slope of 0.85 (R = 0.997). This actually means that in the presence of 2 mol% losartan 6–7 times more cholesterol is needed to induce the same membrane thickening when compared to the pure POPC–Chol bilayer system. Note that $\Delta x/x = (x - x_{pure})/x = 1 - x_{pure}/x = 0.85 \rightarrow x/x_{pure} = 6.6$.

Following this train of thought, losartan has little impact on the DMPC–Chol bilayers. Due to its smaller affinity to the saturated chains as compared to cholesterol, it does not hinder much cholesterol's action. Indeed, this is reflected in the X-ray data: both the bilayer thinning and concentration offset effect of losartan are here much smaller as compared to the situation in POPC–Chol bilayers (Fig. 7). Even worse, the observed formation of MLVs at 40 mol% cholesterol (Fig. 5B) can only be convincingly explained by an almost complete expulsion of losartan from the DMPC–Chol membranes to the aqueous phase. Only in this manner a complete loss of electrostatic repulsion makes really sense (see also the overview Fig. 8C and D). In summary, cholesterol is believed to span the whole hydrophobic part of the membrane monolayer, while losartan's penetration depth in the hydrophobic core is clearly smaller. On the other hand, losartan exhibits a strong affinity to the polar interface by its electrostatic interactions between the negatively charged tetrazole group and surrounding choline groups of the phospholipids. In contrast, in the vicinity of cholesterol the polar phospholipid headgroups are believed to

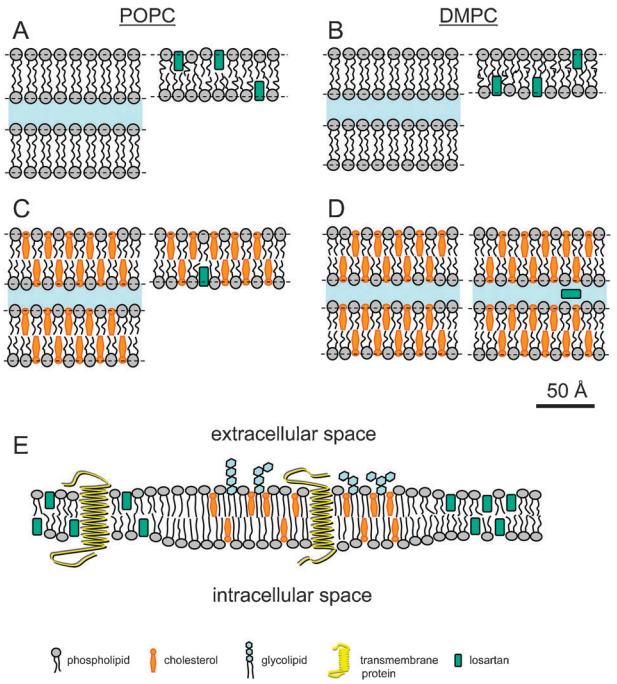

Fig. 8 Structural results overview and scheme of a raft displaying various membrane constituents together with losartan. Schematic illustration of POPC (A) and DMPC (B) bilayer structure alterations induced by losartan. In both cases the up-take of losartan leads to membrane unbinding. The panels A and B refer to Fig. 3 with x_{Los} = 0.2. At very high cholesterol concentrations losartan still finds shelter in the POPC–Chol bilayer (C), whereas it gets expelled from DMPC–Chol membranes (D). The panels C and D refer to Fig. 6 with x_{Chol} = 0.4. A possible scenario for losartan plasma membrane interactions is presented in panel E. Due to the denser lipid packing in the cholesterol rich rafts, losartan is likely to be excluded from this area, and preferentially found in the more fluid plasma membrane regions. Here losartan can accumulate and finally reach the AT_1 receptor site.

act like umbrellas, shielding the non-polar part of cholesterol molecules from water.[47,62]

In the last instance this suggests that losartan is not soluble in highly packed liquid ordered phases in general. Thus, we would expect similar effects for mixtures of long disaturated PCs with cholesterol and in particularly also for mixtures of sphingomyelin with cholesterol, both of which are thought to be enriched in membrane rafts. Therefore one might speculate that losartan encounters a strong energetic barrier, if it must diffuse towards an AT_1R that is embodied in a membrane raft (Fig. 8E). On the general level our results clearly demonstrate that drugs cannot be assumed to partition uniformly into membranes, but may accumulate in certain areas of the membrane. Hence, links between measured blood concentrations of a given drug and membrane concentrations are not as straightforward as supposed usually.[53]

5. Conclusion

Losartan, the forerunner of all non-peptide angiotensin II receptor blockers,[4,9] has been thoroughly studied by SAXS in the fluid phase regime of PCs. Its incorporation into pure phosphatidylcholine bilayers leads to several structural alterations. (i) Due to its strong electronegativity losartan induces already at 2 mol% the unbinding of adjacent membranes. (ii) The bilayer thickness as well as the effective area and volume per molecule reduce with increasing drug concentration. However, the overall bilayer thinning is not big (1–2 Å), and the degree of lipid saturation does not play a big role. (iii) Nevertheless, we could clearly show that losartan displays a significant membrane condensation effect at small drug concentrations, while at higher concentrations partial membrane interdigitation is decisive for the observed decrease in membrane thickness. (iv) From our X-ray data analysis followed a partial area of losartan, $A_{Los} \approx 40$ Å^2.

In a second part, we investigated the influence of losartan on PC–Chol membranes varying the cholesterol concentration from 0–40 mol% and keeping the losartan concentration fixed at 2 mol%. The most important findings are that (i) losartan clearly hampers the induction of the L_o phase, (ii) losartan's ability to suppress the L_o phase is amplified in PC–Chol membranes which contain unsaturated lipids, and (iii) once the L_o phase forms, losartan gets expelled from the bilayer. This is in line with other studies stressing the importance of drug–cholesterol interactions being able to modulate the membrane's phase behavior.[63] In particular, our results suggest that losartan will not preferentially incorporate into densely packed cholesterol–lipid environments as can be expected also for membrane rafts.

References

1 D. Lloyd-Jones, R. J. Adams, T. M. Brown, M. Carnethon, S. Dai, G. De Simone, T. B. Ferguson, E. Ford, K. Furie, C. Gillespie, A. Go, K. Greenlund, N. Haase, S. Hailpern, P. M. Ho, V. Howard, B. Kissela, S. Kittner, D. Lackland, L. Lisabeth, A. Marelli, M. M. McDermott, J. Meigs, D. Mozaffarian, M. Mussolino, G. Nichol, V. L. Roger, W. Rosamond, R. Sacco, P. Sorlie, R. Stafford, T. Thom, S. Wasserthiel-Smoller, N. D. Wong and J. Wylie-Rosett, *Circulation*, 2010, **121**, e46–e215.
2 M. Paul, A. P. Mehr and R. Kreutz, *Physiol. Rev.*, 2006, **86**, 747–803.
3 M. De Gasparo, K. J. Catt, T. Inagami, J. W. Wright and Th. Unger, *Pharmacol. Rev.*, 2000, **52**, 415–472.
4 P. C. Wong, T. B. Barnes, A. T. Chiu, D. D. Christ, J. V. Duncia, W. F. Herblin and P. B. M. W. M. Timmermans, *Cardiovasc. Drug Rev.*, 1991, **9**, 317–339.
5 C. I. Johnston, *Lancet*, 1995, **346**, 1403–1407.
6 L. Tessler and I. Goldberg, *Acta Crystallogr., Sect. E: Struct. Rep. Online*, 2004, **60**, 1830–1832.
7 M. Burnier and H. R. Brunner, *Lancet*, 2000, **355**, 637–645.
8 Z. H. Israili, *J. Hum. Hypertens.*, 2000, **14**, S73–S86.
9 P. B. M. W. Timmermans, P. C. Wong, A. T. Chiu, W. F. Herblin, P. Benfield, D. J. Carini, R. J. Lee, R. R. Wexler, J. A. M. Saye and R. D. Smith, *Pharmacol. Rev.*, 1993, **45**, 205–251.
10 W. B. White, M. A. Weber, D. Sica, G. L. Bakris, A. Perez, C. Cao and S. Kupfer, *Hypertension (Dallas)*, 2011, **57**, 413–420.
11 P. Zoumpoulakis, I. Daliani, M. Zervou, I. Kyrikou, E. Siapi, G. Lamprinidis, E. Mikros and T. Mavromoustakos, *Chem. Phys. Lipids*, 2003, **125**, 13–25.
12 M. Lucio, J. L. F. C. Lima and S. Reis, *Curr. Med. Chem.*, 2010, **17**, 1795–1809.
13 A. M. Seddon, D. Casey, R. V. Law, A. Gee, R. H. Templer and O. Ces, *Chem. Soc. Rev.*, 2009, **38**, 2509–2519.
14 J. Preu, T. Jaeger, V. M. Garamus and T. Gutberlet, *Eur. Biophys. J.*, 2011, **40**, 687–698.
15 T. Mavromoustakos, S. Durdagi, C. Koukoulitsa, M. Simcic, M. G. Papadopoulos, M. Hodoscek and S. G. Grdadolnik, *Curr. Med. Chem.*, 2011, **18**, 2517–2530.

16 E. Theodoropoulou and D. Marsh, *Biochim. Biophys. Acta*, 1999, **1461**, 135–146.
17 C. Potamitis, P. Chatzigeorgiou, E. Siapi, K. Viras, T. Mavromoustakos, A. Hodzic, G. Pabst, F. Cacho-Nerin, P. Laggner and M. Rappolt, *Biochim. Biophys. Acta*, 2011, **1808**, 1753–1763.
18 C. Fotakis, D. Christodouleas, P. Chatzigeorgiou, M. Zervou, N.-P. Benetis, K. Viras and T. Mavromoustakos, *Biophys. J.*, 2009, **96**, 2227–2236.
19 C. Fotakis, S. Gega, E. Siapi, C. Potamitis, K. Viras, P. Moutevelis-Minakakis, C. G. Kokotos, S. Durdagi, S. Golic Grdadolnik, B. Sartori, M. Rappolt and T. Mavromoustakos, *Biochim. Biophys. Acta*, 2010, **1768**, 422–432.
20 E. D. Mantzourani, K. Blokar, T. V. Tselios, J. M. Matsoukas, J. A. Platts, T. M. Mavromoustakos and S. G. Grdadolnik, *Bioorg. Med. Chem.*, 2008, **16**, 2171–2182.
21 C. Fotakis, D. Christodouleas, P. Zoumpoulakis, E. Kritsi, N. P. Benetis, T. Mavromoustakos, H. Reis, A. Gili, M. G. Papadopoulos and M. Zervou, *J. Phys. Chem. B*, 2011, **115**, 6180–6192.
22 P. Zoumpoulakis and T. Mavromoustakos, *Drug Des. Rev.–Online*, 2005, **2**, 537–545.
23 M. A. Bhuiyan, M. Ishiguro, M. Hossain, T. Nakamura, M. Ozaki, S. Miura and T. Nagatomo, *Life Sci.*, 2009, **85**, 136–140.
24 T. Mavromoustakos, P. Chatzigeorgiou, C. Koukoulitsa and S. Durdagi, *Int. J. Quantum Chem.*, 2011, **111**, 1172–1183.
25 D. Ntountaniotis, G. Mali, S. G. Grdadolnik, H. Maria, A.-L. Skaltsounis, C. Potamitis, E. Siapi, P. Chatzigeorgiou, M. Rappolt and T. Mavromoustakos, *Biochim. Biophys. Acta*, 2011, **1808**, 2995–3006.
26 P. Zoumpoulakis, S. G. Grdadolnik, J. M. Matsoukas and T. Mavromoustakos, *J. Pharm. Biomed. Anal.*, 2002, **28**, 125–135.
27 T. Mavromoustakos, A. Kolocouris, M. Zervou, P. Roumelioti, J. M. Matsoukas and R. Weisemann, *J. Med. Chem.*, 1999, **42**, 1714–1722.
28 P. Zoumpoulakis, A. Zoga, P. Roumelioti, N. Giatas, S. G. Grdadolnik, E. Iliodromitis, D. Vlahakos, D. Kremastinos, J. M. Matsoukas and T. Mavromoustakos, *J. Pharm. Biomed. Anal.*, 2003, **31**, 833–844.
29 T. Mavromoustakos, M. Zervou, P. Zoumpoulakis, I. Kyrikou, N. P. Benetis, L. Polevaya, P. Roumelioti, N. Giatas, A. Zoga, P. M. Minakakis, A. Kolocouris, D. Vlahakos, S. G. Grdadolnik and J. M. Matsoukas, *Curr. Top. Med. Chem. (Sharjah, United Arab Emirates)*, 2004, **4**, 385–401.
30 S. Oparil, D. Williams, S. G. Chrysant, T. C. Marbury and J. Neutel, *J. Clin. Hypertens. (Hoboken, NJ, U. S.)*, 2001, **3**, 283–318.
31 T. R. Oliveira, M. T. Lamy, U. M. De Paula, L. L. Guimaraes, M. S. Toledo, H. K. Takahashi, A. H. Straus, C. J. Lindsey and T. B. Paiva, *Braz. J. Med. Biol. Res.*, 2009, **42**, 844–853.
32 T. P. McMullen and R. N. McElhaney, *Biochim. Biophys. Acta*, 1995, **1234**, 90–98.
33 A. Hodzic, M. Rappolt, H. Amenitsch, P. Laggner and G. Pabst, *Biophys. J.*, 2008, **94**, 3935–3944.
34 L. Finegold, *Cholesterol in membrane models*, CRC Press, Baco Raton, FL, 1993.
35 M. R. Vist and J. H. Davis, *Biochemistry*, 1990, **29**, 451–464.
36 D. Marsh, *Biochim. Biophys. Acta*, 2010, **1798**, 688–699.
37 D. Lingwood and K. Simons, *Science*, 2010, **327**, 46–50.
38 H. Amenitsch, M. Rappolt, M. Kriechbaum, H. Mio, P. Laggner and S. Bernstorff, *J. Synchrotron Radiat.*, 1998, **5**, 506–508.
39 G. Pabst, M. Rappolt, H. Amenitsch and P. Laggner, *Phys. Rev. E*, 2000, **62**, 4000–4009.
40 G. Pabst, J. Katsaras, V. A. Raghunathan and M. Rappolt, *Langmuir*, 2003, **19**, 1716–1722.
41 G. Pabst, *Biophys. Rev. Lett.*, 2006, **1**, 57–84.
42 M. Rappolt and G. Pabst, in *Structure and dynamics of membranous interfaces*, ed. K. Nag, John Wiley & Sons, Hoboken, 2008, pp. 45–81.
43 H. I. Petrache and M. F. Brown, in *Methods in Membrane Lipids*, ed. A. Dopico, Humana Press, 2007, pp. 341–353.
44 M. Rappolt, *J. Appl. Phys.*, 2010, **107**, 084701.
45 J. F. Nagle and S. Tristram-Nagle, in *Lipid bilayers. Structure and interactions*, ed. J. Katsaras and T. Gutberlet, Springer, Berlin, 2000, pp. 1–23.
46 J. F. Nagle and S. Tristram-Nagle, *Biochim. Biophys. Acta*, 2000, **1469**, 159–195.
47 S. W. Chiu, E. Jakobsson, R. J. Mashl and H. L. Scott, *Biophys. J.*, 2002, **83**, 1842–1853.
48 A. I. Greenwood, S. Tristram-Nagle and J. F. Nagle, *Chem. Phys. Lipids*, 2006, **143**, 1–10.
49 G. Pabst, A. Hodzic, J. Strancar, S. Danner, M. Rappolt and P. Laggner, *Biophys. J.*, 2007, **93**, 2688–2696.
50 G. Pabst, H. Amenitsch, D. P. Kharakoz, P. Laggner and M. Rappolt, *Phys. Rev. E*, 2004, **70**, 021908.
51 M. R. Brzustowicz and A. T. Brunger, *J. Appl. Crystallogr.*, 2005, **38**, 126–131.
52 N. Kucerka, M. A. Kiselev and P. Balgavy, *Eur. Biophys. J.*, 2004, **33**, 328–334.
53 P. Tosco, B. Rolando, R. Fruttero, Y. Henchoz, S. Martel, P. A. Carrupt and A. Gasco, *Helv. Chim. Acta*, 2008, **91**, 468–482.
54 E. Cagigal, L. Gonzalez, R. M. Alonso and R. M. Jimenez, *J. Pharm. Biomed. Anal.*, 2001, **26**, 477–486.
55 N. Kucerka, S. Tristram-Nagle and J. F. Nagle, *J. Membr. Biol.*, 2005, **208**, 193–202.
56 G. Khelashvili, G. Pabst and D. Harries, *J. Phys. Chem. B*, 2010, **114**, 7524–7534.
57 O. Edholm and J. F. Nagle, *Biophys. J.*, 2005, **89**, 1827–1832.
58 T. Mavromoustakos, P. Zoumpoulakis, I. Kyrikou, A. Zoga, E. Siapi, M. Zervou, I. Daliani, D. Dimitriou, A. Pitsasa, C. Kamoutsis and P. Laggner, *Curr. Top. Med. Chem. (Sharjah, United Arab Emirates)*, 2004, **4**, 445–459.
59 D. Huster and K. Gawrisch, in *Lipid bilayers. Structure and interactions*, ed. J. Katsaras and T. Gutberlet, Springer, Berlin, Heidelberg, New York, 2000, pp. 109–125.
60 M. Meier, X. Li Blatter, A. Seelig and J. Seelig, *Biophys. J.*, 2006, **91**, 2943–2955.
61 M. Rappolt, M. F. Vidal, M. Kriechbaum, M. Steinhart, H. Amenitsch, S. Bernstorff and P. Laggner, *Eur. Biophys. J.*, 2003, **31**, 575–585.
62 J. Huang, J. T. Buboltz and G. W. Feigenson, *Biochim. Biophys. Acta*, 1999, **1417**, 89–100.
63 B. J. Forrest, P. T. P. Linehan and J. Mattai, *Biochemistry*, 1984, **23**, 2288–2293.

